Robotica (2019) volume 37, pp. 233–245. © Cambridge University Press 2018
doi:10.1017/S0263574718000966

High-order singularities of 5R planar parallel robots

Mustafa Özdemir*

Department of Mechanical Engineering, Faculty of Engineering, Marmara University, Göztepe Campus, Kadıköy, Istanbul 34722, Turkey

(Accepted August 25, 2018. First published online: September 20, 2018)

SUMMARY

Singularity analysis of parallel manipulators is an active research field in robotics. The present article derives for the first time in the literature a condition under which a five-bar parallel robot encounters high-order parallel singularities. In this regard, by focusing on the planar 5R mechanism, a theorem is given in terms of the slope of its coupler curve at the parallel singular configurations. At high-order parallel singularities, the associated determinant vanishes simultaneously with at least its first-order time derivative. The determination of such singularities is quite important since in their presence, some special conditions should be satisfied for bounded inverse dynamic solutions.

KEYWORDS: Parallel manipulators, Planar 5R mechanism, Robot dynamics, Singularity, Singularity order

1. Introduction

Closed-loop structure of parallel robots provides higher load-carrying capacity and better positioning accuracy when compared to serial manipulators.[1] Owing to these superiorities, they are being used in a wide range of areas, such as machine tools,[2–4] pick-and-place operations,[5–7] surgery,[8–10] rehabilitation,[11–13] haptic devices,[14–16] motion simulators,[17–19] aerospace applications,[20–22] and painting processes.[23]

However, their closed-loop structure also gives rise to some special kinds of singularities. This is because parallel manipulators possess two Jacobian matrices.[24] Based on these Jacobian matrices, Gosselin and Angeles[25] performed a comprehensive analysis of their singularities. Their analysis has shown that there are three kinds of singularities of a closed-loop mechanism. Among these, the most critical one is "type II",[25] also called "parallel singularities".[26] Near a singularity of this type, the robot becomes, in general, uncontrollable due to the unboundedly growing inverse dynamic solution.[27,28]

Several researchers have studied singularity-free path planning[29,30] and singularity-free zones within the workspace[31–36] of parallel manipulators. However, parallel singularities are usually encountered inside the workspace,[25] and therefore the usable regions of the workspace of parallel robots are mainly small. Actuation redundancy[12,15,16,37–39] and kinematic redundancy[40–42] can be utilized for the avoidance and elimination of singularities. As an alternative solution within the context of redundancy, Parsa et al.[43] proposed to use masses on the robot that are moved by secondary actuators during the crossing of singular points. But, generally speaking, redundant parallel manipulators have some drawbacks, such as additional cost and control complexity.[44] To overcome this additional cost, Agarwal et al.[45] suggested a singularity avoidance control scheme, which is based on controlling only a selected subset of the degrees of freedom of the robot.

There have been also a considerable number of studies on developing methods for non-redundant parallel robots to pass through the singular configurations while preserving the stability of motion.[46–52] The common principle of these works is to plan the motion such that the consistency of the equations of motion of the robot is maintained at the singular position. Ider[46,47] and Jui and Sun[48] formulated

* Corresponding author: E-mail: mustafa.ozdemir@marmara.edu.tr

https://doi.org/10.1017/S0263574718000966 Published online by Cambridge University Press

the linear algebra condition for the existence of infinitely many inverse dynamic solutions at a parallel singularity. Briot and Arakelian[49] worked on the physical interpretation of this condition in terms of wrenches and twists, and on its adaptation and application to flexible manipulators.[50,51] Briot et al.[52] presented some further experimental results on the topic.

Recently, Özdemir[53] has proved that the consistency of the dynamic equations at a parallel singularity is not sufficient alone for the boundedness of the inverse dynamic solution in the neighborhood of that singularity. The novelty of his analysis is in the use of L'Hôpital's Rule to reveal the fact that the time derivatives of the associated vanishing determinant have a fundamental role in the removability of parallel singularities. Based on this, Özdemir[53] has derived the additional conditions necessary for removing singularities from the inverse dynamics of parallel robots. Apart from his aforementioned work,[53] Özdemir[54–56] has also developed balancing and payload placement methods to satisfy the consistency of the equations of motion at parallel singularities not only for any arbitrary path, but also for any arbitrary trajectory. In another very recent paper, Özdemir[57] has also proposed a method to avoid a back-and-forth motion of the end point of the manipulator while passing through the parallel singular configurations. Other than these, singularity-free adjustable designs may be possible for some parallel robots (see, e.g., [58]).

The present article aims to contribute to the literature by deriving, for the first time, a condition under which a five-bar parallel robot encounters high-order parallel singularities. A high-order parallel singularity is characterized by having the associated determinant vanish together with at least its first-order time derivative. A theorem is stated and proved in this regard by focusing on the planar 5R mechanism (where R denotes a revolute joint). Any parallel singularity may or may not be of high order, depending on the desired motion. High-order parallel singularities deserve particular attention since, as previously mentioned, some additional conditions are required for their removal from the inverse dynamic solutions. In order to better understand the importance of analyzing high-order parallel singularities, it will be useful to notice that the constraint forces can be expressed in the form of quotients whose numerators are functions of the parameters and generalized position, velocity and acceleration variables of the mechanism. Their common denominator, on the other hand, is the determinant that vanishes at parallel singularities. The consistency of the dynamic equations guarantees that the numerators also vanish at the singularity time. However, this is not sufficient for ensuring that the constraint forces (and hence the actuator efforts) will have finite limits as the singularity is approached. Their limits may be infinite, depending on how fast the denominator and the numerators go to zero. The aforementioned additional conditions must be satisfied to prevent such an unbounded growth of the inverse dynamic solution.

The rest of the article is organized as follows: Section 2 introduces the notation and some preliminary formulations on the inverse dynamics and parallel singular configurations of the five-bar mechanism. Section 3 defines its high-order parallel singularities by applying L'Hôpital's Rule. Section 4 develops and proves a theorem on the condition for occurrence of its high-order parallel singularities in terms of the slope of its coupler curve. Section 5 presents illustrative examples on the application of the proposed theorem. Section 6 concludes the article.

2. Notation and Preliminaries

Consider a five-bar planar parallel robot with revolute joints (Fig. 1). Because of its wide range of applications,[59] the singularity loci of this robot have been studied by many researchers in the literature.[60–66]

Each moving link has length a_i, mass m_i, and mass moment of inertia I_i about its mass center C_i ($i = 1, 2, 3, 4$). Joints O_1 and O_2 are driven by motor torques τ_1 and τ_2, respectively. The gravitational acceleration, g, acts in the negative y-direction. Point $P(x, y)$ is the coupler point. The dynamic analysis can be started by writing the loop-closure equations as follows:

$$f_1 = a_1 \cos\theta_1 + a_2 \cos(\theta_1 + \theta_2) - a_0 - a_3 \cos\theta_3 - a_4 \cos(\theta_3 + \theta_4) = 0 \quad (1)$$

$$f_2 = a_1 \sin\theta_1 + a_2 \sin(\theta_1 + \theta_2) - a_3 \sin\theta_3 - a_4 \sin(\theta_3 + \theta_4) = 0 \quad (2)$$

https://doi.org/10.1017/S0263574718000966 Published online by Cambridge University Press

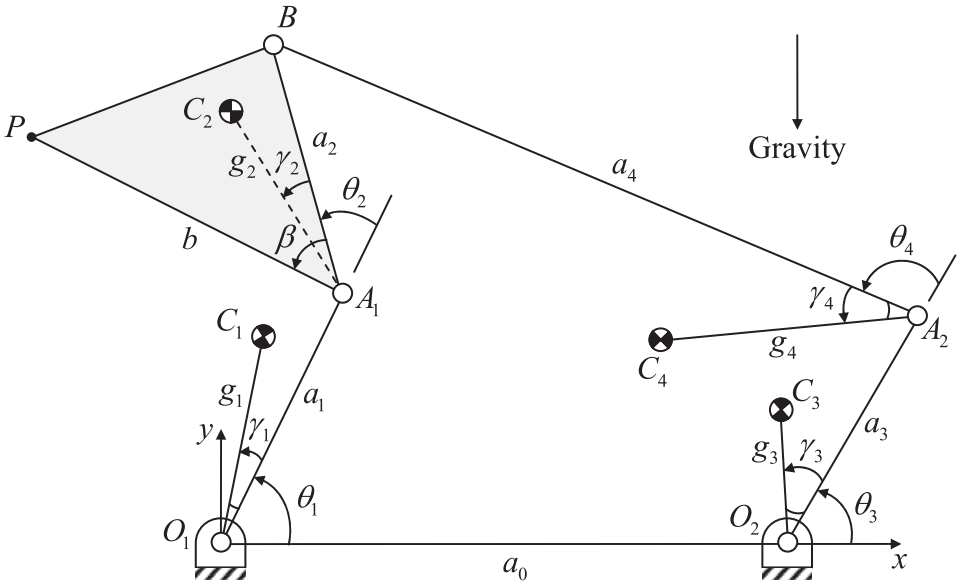


Fig. 1. The 5R planar parallel robot.

where f_1 and f_2 are functions that are used to describe the loop-closure constraints. The Jacobian matrix of these constraint equations is as follows:

$$\mathbf{J} = \begin{bmatrix} J_{11} & J_{21} \\ J_{12} & J_{22} \\ J_{13} & J_{23} \\ J_{14} & J_{24} \end{bmatrix}^T = \begin{bmatrix} -a_1 \sin\theta_1 - a_2 \sin(\theta_1 + \theta_2) & a_1 \cos\theta_1 + a_2 \cos(\theta_1 + \theta_2) \\ -a_2 \sin(\theta_1 + \theta_2) & a_2 \cos(\theta_1 + \theta_2) \\ a_3 \sin\theta_3 + a_4 \sin(\theta_3 + \theta_4) & -a_3 \cos\theta_3 - a_4 \cos(\theta_3 + \theta_4) \\ a_4 \sin(\theta_3 + \theta_4) & -a_4 \cos(\theta_3 + \theta_4) \end{bmatrix}^T \tag{3}$$

Select the generalized coordinates to be the joint variables θ_1, θ_2, θ_3, and θ_4. Then, by using the Lagrangian method, the necessary driving torques for realizing a given task can be expressed as follows:

$$\tau_1 = M_{11}\ddot{\theta}_1 + M_{12}\ddot{\theta}_2 - h_1\left(2\dot{\theta}_1 + \dot{\theta}_2\right)\dot{\theta}_2 + G_1 - J_{11}\lambda_1 - J_{21}\lambda_2 \tag{4}$$

$$\tau_2 = M_{33}\ddot{\theta}_3 + M_{34}\ddot{\theta}_4 - h_2\left(2\dot{\theta}_3 + \dot{\theta}_4\right)\dot{\theta}_4 + G_3 - J_{13}\lambda_1 - J_{23}\lambda_2 \tag{5}$$

where λ_1 and λ_2 are the Lagrange multipliers and they can be determined from the following system of two equations:

$$J_{12}\lambda_1 + J_{22}\lambda_2 = M_{12}\ddot{\theta}_1 + M_{22}\ddot{\theta}_2 + h_1\dot{\theta}_1^2 + G_2 \tag{6}$$

$$J_{14}\lambda_1 + J_{24}\lambda_2 = M_{34}\ddot{\theta}_3 + M_{44}\ddot{\theta}_4 + h_2\dot{\theta}_3^2 + G_4 \tag{7}$$

In the dynamic Eqs. (4)–(7), the coefficients M_{11}, M_{12}, M_{22}, M_{33}, M_{34}, and M_{44} are the elements of the generalized inertia matrix of the robot, the terms including the coefficients h_1 and h_2 are due to the Coriolis and centrifugal effects, and the terms G_1, G_2, G_3, and G_4 are due to the gravity effects. The expressions for these coefficients and terms are given in the Appendix.

While solving Eqs. (6) and (7) for the unknown Lagrange multipliers, singularities occur if the following equation holds:[47,64]

$$D = \begin{vmatrix} J_{12} & J_{22} \\ J_{14} & J_{24} \end{vmatrix} = J_{12}J_{24} - J_{14}J_{22} = a_2 a_4 \sin(\theta_1 + \theta_2 - \theta_3 - \theta_4) = 0 \tag{8}$$

https://doi.org/10.1017/S0263574718000966 Published online by Cambridge University Press

or, equivalently,

$$\theta_1 + \theta_2 - \theta_3 - \theta_4 = k\pi \tag{9}$$

Here, k can be 0 or ± 1. Such configurations of the robot are its parallel singularities.

3. High-Order Parallel Singularities of the 5R Planar Manipulator

It will be convenient to rewrite Eqs. (6) and (7) in the following compact form:

$$\begin{bmatrix} J_{12} & J_{22} \\ J_{14} & J_{24} \end{bmatrix} \begin{bmatrix} \lambda_1 \\ \lambda_2 \end{bmatrix} = \begin{bmatrix} r_1 \\ r_2 \end{bmatrix} \tag{10}$$

where

$$r_1 = M_{12}\ddot{\theta}_1 + M_{22}\ddot{\theta}_2 + h_1\dot{\theta}_1^2 + G_2 \tag{11}$$

$$r_2 = M_{34}\ddot{\theta}_3 + M_{44}\ddot{\theta}_4 + h_2\dot{\theta}_3^2 + G_4 \tag{12}$$

By solving this linear system, one can obtain the Lagrange multipliers as

$$\lambda_1 = \frac{N_1}{D} \tag{13}$$

$$\lambda_2 = \frac{N_2}{D} \tag{14}$$

where

$$N_1 = J_{24}r_1 - J_{22}r_2 \tag{15}$$

$$N_2 = -J_{14}r_1 + J_{12}r_2 \tag{16}$$

At a parallel singularity, the determinant D appearing in the denominators of Eqs. (13) and (14) becomes zero, as also previously mentioned. Thus, the Lagrange multipliers become undefined at such a singular configuration. However, it is still possible to make them and hence the motor torques remain bounded in the neighborhood of the singular position. The necessary conditions for this are as follows:

$$N_1(t_s) = 0 \tag{17}$$

$$N_2(t_s) = 0 \tag{18}$$

where t_s denotes the time at which the parallel singularity occurs. If Eqs. (17) and (18) hold, then the quotients shown in Eqs. (13) and (14) will result in the indeterminate form of type $0/0$. Therefore, L'Hôpital's Rule[67] can be applied to evaluate the limits $\lim_{t\to t_s} \lambda_1(t)$ and $\lim_{t\to t_s} \lambda_2(t)$ as follows:

$$\lim_{t\to t_s} \lambda_1(t) = \lim_{t\to t_s} \frac{N_1(t)}{D(t)} = \lim_{t\to t_s} \frac{\dot{N}_1(t)}{\dot{D}(t)} = \frac{\dot{N}_1(t_s)}{\dot{D}(t_s)} \tag{19}$$

$$\lim_{t\to t_s} \lambda_2(t) = \lim_{t\to t_s} \frac{N_2(t)}{D(t)} = \lim_{t\to t_s} \frac{\dot{N}_2(t)}{\dot{D}(t)} = \frac{\dot{N}_2(t_s)}{\dot{D}(t_s)} \tag{20}$$

In the above equations, t denotes the time variable. At this point, one should notice that the rows of the coefficient matrix shown in Eq. (10) become linearly dependent at a parallel singularity as follows:[47]

$$\begin{bmatrix} J_{14} & J_{24} \end{bmatrix} = \sigma \frac{a_4}{a_2} \begin{bmatrix} J_{12} & J_{22} \end{bmatrix} \tag{21}$$

https://doi.org/10.1017/S0263574718000966 Published online by Cambridge University Press

where $\sigma = 1$ if $k = \pm 1$, and $\sigma = -1$ if $k = 0$. Thus, the "consistency condition" that should be met at the singular position can be expressed as follows:[47]

$$r_2 = \sigma \frac{a_4}{a_2} r_1 \tag{22}$$

If the condition given by Eq. (22) is satisfied, the conditions given by Eqs. (17) and (18) are also simultaneously satisfied. This can be verified by substituting Eqs. (21) and (22) into Eqs. (15) and (16).

However, if the first n time derivatives of D vanish simultaneously at time t_s, then the following additional conditions are also required to be met for the boundedness of the inverse dynamic solution near the singularity:

$$\left.\frac{d^j N_1(t)}{dt^j}\right|_{t=t_s} = 0, \qquad j = 1, \ldots, n \tag{23}$$

$$\left.\frac{d^j N_2(t)}{dt^j}\right|_{t=t_s} = 0, \qquad j = 1, \ldots, n \tag{24}$$

Once these additional conditions are also satisfied, the limits $\lim_{t\to t_s} \lambda_1(t)$ and $\lim_{t\to t_s} \lambda_2(t)$ will be finite and L'Hôpital's Rule can be applied successively to evaluate them. Otherwise, the inverse dynamic solution will grow unbounded as the singularity is approached. It is also worth to mention that if the said limits are guaranteed to be finite, then the singularity can be removed by setting $\lambda_1(t_s) = \lim_{t\to t_s} \lambda_1(t)$ and $\lambda_2(t_s) = \lim_{t\to t_s} \lambda_2(t)$. Hence, the inverse dynamic solution becomes continuous and bounded. Interested readers are invited to see also the singularity removal theorems proposed by Özdemir in ref. [53] in terms of a set of functions called "Mu functions".

4. A Theorem on the Slope of the Coupler Curve at a High-Order Parallel Singularity

Below, a theorem is developed and proved to give the condition for the planar 5R mechanism to have a high-order parallel singularity. The section is finished with a remark concerning the case where the mechanism comes to an instantaneous rest at a parallel singular configuration.

Theorem. Consider the 5R planar parallel robot as shown in Fig. 1. Let the base joints be the actuated joints. Let further the point $P(x, y)$ be the coupler point. At least the first-order time derivative of the determinant D is also zero at a parallel singular configuration if the slope of the coupler curve at that configuration is

$$\frac{dy}{dx} = -\frac{a_2 \cos\theta_1 \sin(\theta_1 + \theta_2 - \theta_3) - a_4 \cos\theta_1 \sin\theta_4 - b\cos(\theta_1 + \theta_2 + \beta)\sin(\theta_1 - \theta_3)}{a_2 \sin\theta_1 \sin(\theta_1 + \theta_2 - \theta_3) - a_4 \sin\theta_1 \sin\theta_4 - b\sin(\theta_1 + \theta_2 + \beta)\sin(\theta_1 - \theta_3)}$$

Proof: One can write the first time derivative of the determinant D as follows:

$$\dot{D} = a_2 a_4 \left(\dot{\theta}_1 + \dot{\theta}_2 - \dot{\theta}_3 - \dot{\theta}_4\right) \cos(\theta_1 + \theta_2 - \theta_3 - \theta_4) \tag{25}$$

Recall that at a parallel singularity, the determinant D becomes zero. Since sine and cosine of an angle cannot vanish simultaneously, $\dot{D}$ can simultaneously become zero at a parallel singularity if and only if the following equation holds at that singular position:

$$\dot{\theta}_1 + \dot{\theta}_2 - \dot{\theta}_3 - \dot{\theta}_4 = 0 \tag{26}$$

Differentiating Eqs. (1) and (2) gives

$$J_{11}\dot{\theta}_1 + J_{12}\dot{\theta}_2 + J_{13}\dot{\theta}_3 + J_{14}\dot{\theta}_4 = 0 \tag{27}$$

$$J_{21}\dot{\theta}_1 + J_{22}\dot{\theta}_2 + J_{23}\dot{\theta}_3 + J_{24}\dot{\theta}_4 = 0 \tag{28}$$

https://doi.org/10.1017/S0263574718000966 Published online by Cambridge University Press

The coordinates of the coupler point $P(x, y)$ can be expressed as follows:

$$x = a_1 \cos\theta_1 + b \cos(\theta_1 + \theta_2 + \beta) \tag{29}$$

$$y = a_1 \sin\theta_1 + b \sin(\theta_1 + \theta_2 + \beta) \tag{30}$$

Differentiating Eqs. (29) and (30) yields

$$\dot{x} = \Phi_{11}\dot{\theta}_1 + \Phi_{12}\dot{\theta}_2 \tag{31}$$

$$\dot{y} = \Phi_{21}\dot{\theta}_1 + \Phi_{22}\dot{\theta}_2 \tag{32}$$

where

$$\Phi_{11} = -a_1 \sin\theta_1 - b \sin(\theta_1 + \theta_2 + \beta) \tag{33}$$

$$\Phi_{12} = -b \sin(\theta_1 + \theta_2 + \beta) \tag{34}$$

$$\Phi_{21} = a_1 \cos\theta_1 + b \cos(\theta_1 + \theta_2 + \beta) \tag{35}$$

$$\Phi_{22} = b \cos(\theta_1 + \theta_2 + \beta) \tag{36}$$

By the use of Eqs. (27), (28), (31), and (32), one can obtain

$$\dot{\theta}_1 = \frac{1}{\Delta_1}(\Phi_{22}\dot{x} - \Phi_{12}\dot{y}) \tag{37}$$

$$\dot{\theta}_2 = -\frac{1}{\Delta_1}(\Phi_{21}\dot{x} - \Phi_{11}\dot{y}) \tag{38}$$

$$\dot{\theta}_3 = \frac{1}{\Delta_1\Delta_2}\left[(D\Phi_{21} - \delta_1\Phi_{22})\dot{x} - (D\Phi_{11} - \delta_1\Phi_{12})\dot{y}\right] \tag{39}$$

$$\dot{\theta}_4 = -\frac{1}{\Delta_1\Delta_2}\left[(\delta_2\Phi_{21} - \delta_3\Phi_{22})\dot{x} - (\delta_2\Phi_{11} - \delta_3\Phi_{12})\dot{y}\right] \tag{40}$$

where

$$\Delta_1 = \Phi_{11}\Phi_{22} - \Phi_{12}\Phi_{21} = a_1 b \sin(\theta_2 + \beta) \tag{41}$$

$$\Delta_2 = J_{13}J_{24} - J_{14}J_{23} = a_3 a_4 \sin\theta_4 \tag{42}$$

$$\delta_1 = J_{11}J_{24} - J_{14}J_{21} = D + a_1 a_4 \sin(\theta_1 - \theta_3 - \theta_4) \tag{43}$$

$$\delta_2 = J_{12}J_{23} - J_{13}J_{22} = D + a_2 a_3 \sin(\theta_1 + \theta_2 - \theta_3) \tag{44}$$

$$\delta_3 = J_{11}J_{23} - J_{13}J_{21} = D + a_1 a_3 \sin(\theta_1 - \theta_3) + a_2 a_3 \sin(\theta_1 + \theta_2 - \theta_3) + a_1 a_4 \sin(\theta_1 - \theta_3 - \theta_4) \tag{45}$$

As can be understood from Eqs. (37)–(40), the configurations where $\Delta_1 = 0$ or $\Delta_2 = 0$ correspond to "type I singularities"[25] or "serial singularities"[26] of the robot, which are out of the scope of this article.

On substituting Eqs. (8) and (37)–(40) into Eq. (26), one gets

$$\psi_1\dot{x} + \psi_2\dot{y} = 0 \tag{46}$$

https://doi.org/10.1017/S0263574718000966 Published online by Cambridge University Press

where

$$\psi_1 = \frac{a_2 \cos\theta_1 \sin(\theta_1 + \theta_2 - \theta_3) - a_4 \cos\theta_1 \sin\theta_4 - b\cos(\theta_1 + \theta_2 + \beta)\sin(\theta_1 - \theta_3)}{a_4 b \sin(\theta_2 + \beta)\sin\theta_4} \tag{47}$$

$$\psi_2 = \frac{a_2 \sin\theta_1 \sin(\theta_1 + \theta_2 - \theta_3) - a_4 \sin\theta_1 \sin\theta_4 - b\sin(\theta_1 + \theta_2 + \beta)\sin(\theta_1 - \theta_3)}{a_4 b \sin(\theta_2 + \beta)\sin\theta_4} \tag{48}$$

One can conclude from Eq. (46) that the first-order time derivative of the determinant D is also zero at a parallel singularity if the slope of the coupler curve at that singular position is

$$\frac{dy}{dx} = \frac{\dot{y}}{\dot{x}} = -\frac{\psi_1}{\psi_2} = -\frac{a_2\cos\theta_1\sin(\theta_1 + \theta_2 - \theta_3) - a_4\cos\theta_1\sin\theta_4 - b\cos(\theta_1 + \theta_2 + \beta)\sin(\theta_1 - \theta_3)}{a_2\sin\theta_1\sin(\theta_1 + \theta_2 - \theta_3) - a_4\sin\theta_1\sin\theta_4 - b\sin(\theta_1 + \theta_2 + \beta)\sin(\theta_1 - \theta_3)} \tag{49}$$

That completes the proof. **Q.E.D.**

Remark. As should be clear from Eq. (46), the first-order time derivative of the determinant D becomes also zero at a parallel singularity if the planar 5R robot comes instantaneously to rest at that singular position, i.e., if $\dot{x}(t_s) = \dot{y}(t_s) = 0$.

5. Numerical Examples

This section gives examples to illustrate how the same parallel singular configuration may or may not be of high order, depending on the slope of the coupler curve at that configuration. The values of the mechanism parameters are arbitrarily chosen as follows: $a_0 = 4$ m, $a_1 = a_3 = 2$ m, $a_2 = a_4 = b = 3$ m, and $\beta = 0$.

As a first example, consider a desired motion of the coupler point along a vertical straight-line segment between the initial point $P_0(x_0, y_0) = P_0(2, 1.232)$ and the final point $P_f(x_f, y_f) = P_f(2, 2.232)$. Notice that $x_0 = x_f$. The motion is to be completed in $t_f = 2$ s. This path can be parameterized as follows:

$$x(t) = x_0 \tag{50}$$

$$y(t) = y_0 + f(t) \tag{51}$$

where f is a time function such that

$$f(0) = 0 \tag{52}$$

$$f(t_f) = y_f - y_0 \tag{53}$$

Additionally, the robot is required to have zero initial and final velocities and accelerations, i.e.,

$$\dot{f}(0) = 0 \tag{54}$$

$$\dot{f}(t_f) = 0 \tag{55}$$

$$\ddot{f}(0) = 0 \tag{56}$$

$$\ddot{f}(t_f) = 0 \tag{57}$$

Thus, the following fifth-order polynomial can be used for f to satisfy the six task requirements given by Eqs. (52)–(57):

$$f(t) = 1.25t^3 - 0.9375t^4 + 0.1875t^5 \tag{58}$$

This linear path is free of serial singularities. However, a parallel singular configuration occurs (i.e., the determinant D becomes zero) when the coupler point comes to $P_s(x_s, y_s) = P_s(2, 1.732)$ at $t_s = 1$ s (Fig. 2). The values of the joint variables at this singular configuration can be found as follows: $\theta_1 = \theta_4 = 120^\circ$, $\theta_2 = 240^\circ$, and $\theta_3 = 60^\circ$ (a sketch of the mechanism at this singular configuration

https://doi.org/10.1017/S0263574718000966 Published online by Cambridge University Press

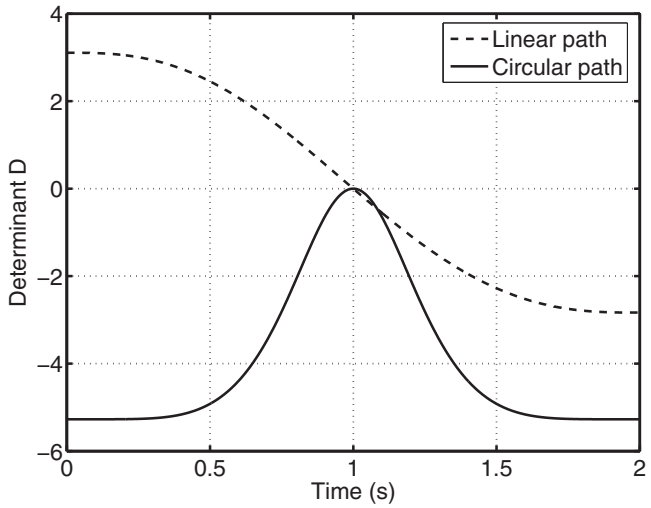


Fig. 2. Determinants associated with parallel singularities.

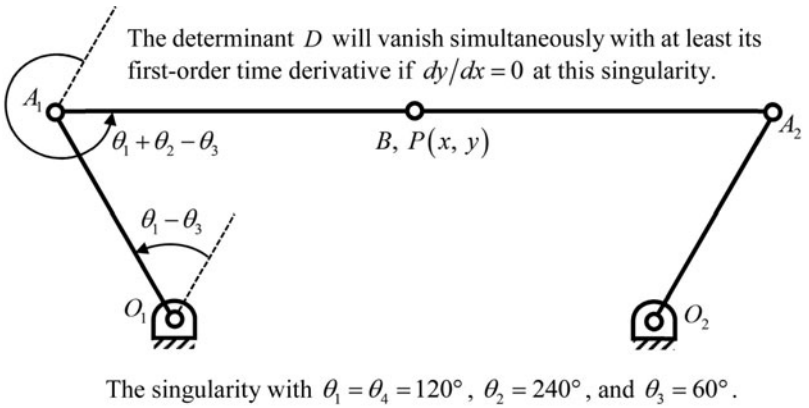


Fig. 3. The parallel singular configuration encountered.

is shown in Fig. 3). Note also that $\dot{y}(t_s) = 0.9375$ m/s. Hence, the mechanism does not come to an instantaneous rest at the singularity. The proposed theorem can therefore be used to conclude that the slope of the coupler curve should be zero (i.e., the tangent line to the coupler curve should be horizontal) at this configuration for a high-order parallel singularity to occur. Recall, however, that the path is a vertical straight-line segment. Due to these reasons, the determinant D has a nonzero first-order time derivative at the singular position, as can be seen in Fig. 2. Consider now, for a second example, a circle which is centered at $Q(x_Q, y_Q) = Q(2, 2.232)$ and has a radius of $\rho = 0.5$ m. The coupler point will make a full rotation along this circle in counterclockwise direction, starting from $P_0(x_0, y_0) = P_0(2, 2.732)$. The motion starts and finishes with zero velocity and acceleration. The duration of the task is $t_f = 2$ s. These task specifications can be fulfilled by the following equations:

$$x(t) = x_Q + \rho \cos\alpha(t) \tag{59}$$

$$y(t) = y_Q + \rho \sin\alpha(t) \tag{60}$$

where

$$\alpha(t) = \frac{\pi}{2}\left(1 + 5t^3 - \frac{15}{4}t^4 + \frac{3}{4}t^5\right) \tag{61}$$

Again, no serial singularity is encountered during the realization of this circular path. But the same parallel singular configuration occurs at the same time (Fig. 2). Moreover, the robot is similarly in

https://doi.org/10.1017/S0263574718000966 Published online by Cambridge University Press

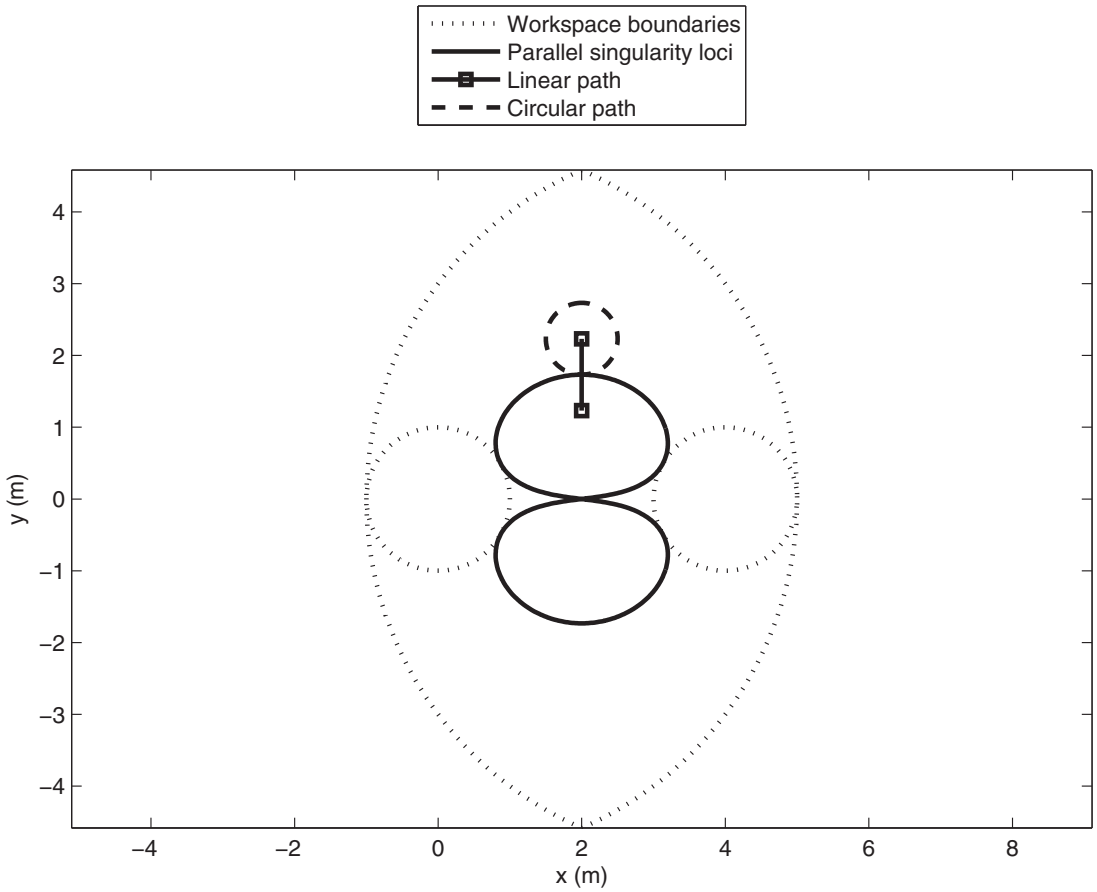


Fig. 4. Workspace boundaries and parallel singularity loci of the robot together with the considered linear and circular paths.

motion at this instant with $\dot{x}(t_s) = 2.945$ m/s. However, the determinant D and its first time derivative vanish simultaneously at the singular configuration, as can be seen in Fig. 2, since the slope of the coupler curve is horizontal at this configuration. Thus, the singular configuration of interest becomes of high order with the considered circular path.

Finally, in order to gain further insights into high-order parallel singularities, the considered linear and circular paths, and the parallel singularity loci are superimposed on the workspace of the robot as shown in Fig. 4. It can be clearly seen from this figure that both paths pass through the same singular point. However, the circular path and the singularity loci curve have the same tangent line at this point, i.e., the circular path and the singularity loci curve are tangent to each other.

6. Conclusions

This article derives, for the first time in the literature, a condition under which a five-bar parallel robot encounters a high-order parallel singularity. By concentrating on the planar 5R mechanism, which is one of the most widely used mechanisms in industrial applications, it is shown that for certain slopes of the coupler curve at parallel singular configurations, the associated determinant vanishes simultaneously with at least its first-order time derivative. The developed method for the determination of high-order parallel singularities of the mechanism is important in that some additional conditions are needed for their removal from the inverse dynamic solutions.

To conclude, this study leads to new insights into the classical problem of singularities of parallel robots, which has been under extensive research for more than two decades. The analysis performed here can be easily adapted and extended for various parallel manipulators. To discuss this, consider a parallel robot with F degrees of freedom. This closed-loop kinematic chain can be converted into a tree-structure open kinematic chain by virtually cutting a sufficient number of passive joints. Let N

https://doi.org/10.1017/S0263574718000966 Published online by Cambridge University Press

be the degrees of freedom of the open kinematic chain. Let further the vector of joint variables of the open tree structure be denoted by $\mathbf{q} = [\, q_1 \; q_2 \; \ldots \; q_N \,]^T$. Without loss of generality, the elements of $\mathbf{q}$ are assumed to be ordered such that the first F are the actuated joint variables and the last $N - F$ are the variables of the passive joints. The vector of generalized coordinates can be chosen as $\mathbf{q}$. The $N - F$ loop-closure constraints can be represented as the following system of equations:

$$\begin{array}{c} f_1(\mathbf{q}) = 0 \\ f_2(\mathbf{q}) = 0 \\ \vdots \\ f_{N-F}(\mathbf{q}) = 0 \end{array} \tag{62}$$

Following Refs. [47] and [64], the determinant that vanishes at parallel singularities can be written as

$$D(\mathbf{q}) = \begin{vmatrix} \dfrac{\partial f_1}{\partial q_{F+1}} & \dfrac{\partial f_2}{\partial q_{F+1}} & \cdots & \dfrac{\partial f_{N-F}}{\partial q_{F+1}} \\ \dfrac{\partial f_1}{\partial q_{F+2}} & \dfrac{\partial f_2}{\partial q_{F+2}} & \cdots & \dfrac{\partial f_{N-F}}{\partial q_{F+2}} \\ \vdots & \vdots & & \vdots \\ \dfrac{\partial f_1}{\partial q_N} & \dfrac{\partial f_2}{\partial q_N} & \cdots & \dfrac{\partial f_{N-F}}{\partial q_N} \end{vmatrix} \tag{63}$$

The determinant D will vanish together with its first-order time derivative if the generalized velocities $\dot{q}_1, \dot{q}_2, \ldots, \dot{q}_N$ satisfy the following relation at the singular configuration:

$$\frac{\partial D}{\partial q_1}\dot{q}_1 + \frac{\partial D}{\partial q_2}\dot{q}_2 + \cdots + \frac{\partial D}{\partial q_N}\dot{q}_N = 0 \tag{64}$$

References

1. J.-P. Merlet, *Parallel Robots*, 2nd ed. (Springer, Dordrecht, The Netherlands, 2006).
2. L. Wang, J. Wu, J. Wang and Z. You, "An experimental study of a redundantly actuated parallel manipulator for a 5-DOF hybrid machine tool," *IEEE-ASME Trans. Mechatron.* **14**(1), 72–81 (2009).
3. L. Wang, J. Wu, T. Li, J. Wang and G. Gao, "A study on the dynamic characteristics of the 2-DOF redundant parallel manipulator of a hybrid machine tool," *Int. J. Robot. Autom.* **30**(2), 184–191 (2015).
4. S. F. M. Assal, "A novel planar parallel manipulator with high orientation capability for a hybrid machine tool: Kinematics, dimensional synthesis and performance evaluation," *Robotica* **35**(5), 1031–1053 (2017).
5. A. Joubair, M. Slamani and I. A. Bonev, "Kinematic calibration of a five-bar planar parallel robot using all working modes," *Robot. Comput.-Integr. Manuf.* **29**(4), 15–25 (2013).
6. F. Bourbonnais, P. Bigras and I. A. Bonev, "Minimum-time trajectory planning and control of a pick-and-place five-bar parallel robot," *IEEE-ASME Trans. Mechatron.* **20**(2), 740–749 (2015).
7. J. Mo, Z.-F. Shao, L. Guan, F. Xie and X. Tang, "Dynamic performance analysis of the X4 high-speed pick-and-place parallel robot," *Robot. Comput.-Integr. Manuf.* **46**, 48–57 (2017).
8. D. Pisla, B. Gherman, C. Vaida, M. Suciu and N. Plitea, "An active hybrid parallel robot for minimally invasive surgery," *Robot. Comput.-Integr. Manuf.* **29**(4), 203–221 (2013).
9. M. M. Dalvand and B. Shirinzadeh, "Motion control analysis of a parallel robot assisted minimally invasive surgery/microsurgery system (PRAMiSS)," *Robot. Comput.-Integr. Manuf.* **29**(2), 318–327 (2013).
10. K. Ibrahim, A. Ramadan, M. Fanni, Y. Kobayashi, A. Abo-Ismail and M. G. Fujie, "Development of a new 4-DOF endoscopic parallel manipulator based on screw theory for laparoscopic surgery," *Mechatronics* **28**, 4–17 (2015).
11. Z. M. Bi, "Design of a spherical parallel kinematic machine for ankle rehabilitation," *Adv. Robot.* **27**(2), 121–132 (2013).
12. C. Wang, Y. Fang, S. Guo and C. Zhou, "Design and kinematic analysis of redundantly actuated parallel mechanisms for ankle rehabilitation," *Robotica* **33**(2), 366–384 (2015).
13. S. Mohan, J. K. Mohanta, S. Kurtenbach, J. Paris, B. Corves and M. Huesing, "Design, development and control of a 2PRP-2PPR planar parallel manipulator for lower limb rehabilitation therapies," *Mech. Mach. Theory* **112**, 272–294 (2017).

https://doi.org/10.1017/S0263574718000966 Published online by Cambridge University Press

14. J. W. Yoon, J. Ryu and Y.-K. Hwang, "Optimum design of 6-DOF parallel manipulator with translational/rotational workspaces for haptic device application," *J. Mech. Sci. Technol.* **24**(5), 1151–1162 (2010).
15. H. Saafi, M. A. Laribi and S. Zeghloul, "Redundantly actuated 3-RRR spherical parallel manipulator used as a haptic device: Improving dexterity and eliminating singularity," *Robotica* **33**(5), 1113–1130 (2015).
16. H. Saafi, M. A. Laribi, and S. Zeghloul, "Optimal torque distribution for a redundant 3-RRR spherical parallel manipulator used as a haptic medical device," *Robot. Auton. Syst.* **89**, 40–50 (2017).
17. B. Dasgupta and T. S. Mruthyunjaya, "The Stewart platform manipulator: A review," *Mech. Mach. Theory* **35**(1), 15–40 (2000).
18. J. Zhang, F. Gao, H. Yu and X. Zhao, "Use of an orthogonal parallel robot with redundant actuation as an earthquake simulator and its experiments," *Proc. Inst. Mech. Eng. Part C-J. Eng. Mech. Eng. Sci.* **226**(1), 257–272 (2012).
19. C. Zhang and L. Zhang, "Kinematics analysis and workspace investigation of a novel 2-DOF parallel manipulator applied in vehicle driving simulator," *Robot. Comput.-Integr. Manuf.* **29**(4), 113–120 (2013).
20. S. H. Lee, B.-J. Yi, S. H. Kim and Y. K. Kwak, "Modeling and analysis on the internal impact of a Stewart platform utilized for spacecraft docking," *Adv. Robot.* **15**(7), 763–777 (2001).
21. A. Omran and A. Kassem, "Optimal task space control design of a Stewart manipulator for aircraft stall recovery," *Aerosp. Sci. Technol.* **15**(5), 353–365 (2011).
22. Y. Song, Y. Qi, G. Dong and T. Sun, "Type synthesis of 2-DoF rotational parallel mechanisms actuating the inter-satellite link antenna," *Chin. J. Aeronaut.* **29**(6), 1795–1805 (2016).
23. J. Wu, Y. Gao, B. Zhang and L. Wang, "Workspace and dynamic performance evaluation of the parallel manipulators in a spray-painting equipment," *Robot. Comput.-Integr. Manuf.* **44**, 199–207 (2017).
24. J. Angeles, *Fundamentals of Robotic Mechanical Systems: Theory, Methods, and Algorithms*, 4th ed. (Springer International Publishing, Switzerland, 2014).
25. C. Gosselin and J. Angeles, "Singularity analysis of closed-loop kinematic chains," *IEEE Trans. Robot. Autom.* **6**(3), 281–290 (1990).
26. J.-P. Merlet and C. Gosselin, "Parallel Mechanisms and Robots," **In:** *Springer Handbook of Robotics* (B. Siciliano and O. Khatib, eds.), (Springer-Verlag Berlin Heidelberg. Würzburg, 2008) pp. 269–285.
27. Y. Takeda and H. Funabashi, "Kinematic and static characteristics of in-parallel actuated manipulators at singular points and in their neighborhood," *JSME Int. J. Ser. C-Dyn. Control Robot. Des. Manuf.* **39**(1), 85–93 (1996).
28. P. Choudhury and A. Ghosal, "Singularity and controllability analysis of parallel manipulators and closed-loop mechanisms," *Mech. Mach. Theory* **35**(10), 1455–1479 (2000).
29. A. K. Dash, I.-M. Chen, S. H. Yeo and G. Yang, "Workspace generation and planning singularity-free path for parallel manipulators," *Mech. Mach. Theory* **40**(7), 776–805 (2005).
30. B. Li, K. Wang, Y. Han, Y. Cao, H. Yang and S. Liu, "Singularity property and singularity-free path planning of the Gough–Stewart parallel mechanism," *Int. J. Adv. Robot. Syst.* **14**(6), (2017).
31. H. Li, C. M. Gosselin and M. J. Richard, "Determination of maximal singularity-free zones in the workspace of planar three-degree-of-freedom parallel mechanisms," *Mech. Mach. Theory* **41**(10), 1157–1167 (2006).
32. H. Li, C. M. Gosselin and M. J. Richard, "Determination of the maximal singularity-free zones in the six-dimensional workspace of the general Gough–Stewart platform," *Mech. Mach. Theory* **42**(4), 497–511 (2007).
33. M. A. Mousavi, M. T. Masouleh and A. Karimi, "On the maximal singularity-free ellipse of planar 3-RPR parallel mechanisms via convex optimization," *Robot. Comput.-Integr. Manuf.* **30**(2), 218–227 (2014).
34. M. H. F. Kaloorazi, M. T. Masouleh and S. Caro, "Determining the maximal singularity-free circle or sphere of parallel mechanisms using interval analysis," *Robotica* **34**(1), 135–149 (2016).
35. Y. Liu, J. Wu, L. Wang and J. Wang "Determination of the maximal singularity-free zone of 4-RRR redundant parallel manipulators and its application on investigating length ratios of links," *Robotica* **34**(9), 2039–2055 (2016).
36. A. Nayak, L. Nurahmi, P. Wenger and S. Caro, "Comparison of 3-RPS and 3-SPR parallel manipulators based on their maximum inscribed singularity-free circle," **In:** *New Trends in Mechanism and Machine Science: Theory and Industrial Applications* (P. Wenger and P. Flores, eds.) (Springer International Publishing, Switzerland, 2017) pp. 121–130.
37. B. Dasgupta and T. S. Mruthyunjaya, "Force redundancy in parallel manipulators: Theoretical and practical issues," *Mech. Mach. Theory* **33**(6), 727–742 (1998).
38. J. A. Saglia, J. S. Dai and D. G. Caldwell, "Geometry and kinematic analysis of a redundantly actuated parallel mechanism that eliminates singularities and improves dexterity," *J. Mech. Des.* **130**(12), 124501 (2008).
39. S. Li, Y. Liu, H. Cui, Y. Niu and Y. Zhao, "Synthesis of branched chains with actuation redundancy for eliminating interior singularities of 3T1R parallel mechanisms," *Chin. J. Mech. Eng.* **29**(2), 250–259 (2016).
40. S.-H. Cha, T. A. Lasky and S. A. Velinsky, "Determination of the kinematically redundant active prismatic joint variable ranges of a planar parallel mechanism for singularity-free trajectories," *Mech. Mach. Theory* **44**(5), 1032–1044 (2009).
41. C. Gosselin, T. Laliberté and A. Veillette, "Singularity-free kinematically redundant planar parallel mechanisms with unlimited rotational capability," *IEEE Trans. Robot.* **31**(2), 457–467 (2015).

https://doi.org/10.1017/S0263574718000966 Published online by Cambridge University Press

42. C. Gosselin and L.-T. Schreiber, "Kinematically redundant spatial parallel mechanisms for singularity avoidance and large orientational workspace," *IEEE Trans. Robot.* **32**(2), 286–300 (2016).
43. S. S. Parsa, R. Boudreau and J. A. Carretero, "Reconfigurable mass parameters to cross direct kinematic singularities in parallel manipulators," *Mech. Mach. Theory* **85**, 53–63 (2015).
44. M. Luces, J. K. Mills and B. Benhabib, "A review of redundant parallel kinematic mechanisms," *J. Intell. Robot. Syst.* **86**(2), 175–198 (2017).
45. A. Agarwal, C. Nasa and S. Bandyopadhyay, "Dynamic singularity avoidance for parallel manipulators using a task-priority based control scheme," *Mech. Mach. Theory* **96**, Part 1, 107–126 (2016).
46. S. K. Ider, "Singularity robust inverse dynamics of planar 2-RPR parallel manipulators," *Proc. Inst. Mech. Eng. Part C-J. Eng. Mech. Eng. Sci.* **218**(7), 721–730 (2004).
47. S. K. Ider, "Inverse dynamics of parallel manipulators in the presence of drive singularities," *Mech. Mach. Theory* **40**(1), 33–44 (2005).
48. C. K. K. Jui and Q. Sun, "Path tracking of parallel manipulators in the presence of force singularity," *J. Dyn. Syst. Meas. Control-Trans. ASME* **127**(4), 550–563 (2005).
49. S. Briot and V. Arakelian, "Optimal force generation in parallel manipulators for passing through the singular positions," *Int. J. Robot. Res.* **27**(8), 967–983 (2008).
50. S. Briot and V. Arakelian, "On the dynamic properties of rigid-link flexible-joint parallel manipulators in the presence of type 2 singularities," *J. Mech. Robot.* **2**(2), 021004 (2010).
51. S. Briot and V. Arakelian, "On the dynamic properties of flexible parallel manipulators in the presence of type 2 singularities," *J. Mech. Robot.* **3**(3), 031009 (2011).
52. S. Briot, G. Pagis, N. Bouton and P. Martinet, "Degeneracy conditions of the dynamic model of parallel robots," *Multibody Syst. Dyn.* **37**(4), 371–412 (2016).
53. M. Özdemir, "Removal of singularities in the inverse dynamics of parallel robots," *Mech. Mach. Theory* **107**, 71–86 (2017).
54. M. Özdemir, "Singularity robust balancing of parallel manipulators following inconsistent trajectories," *Robotica* **34**(9), 2027–2038 (2016).
55. M. Özdemir, "Singularity-consistent payload locations for parallel manipulators," *Mech. Mach. Theory* **97**, 171–189 (2016).
56. M. Özdemir, "Dynamic analysis of planar parallel robots considering singularities and different payloads," *Robot. Comput.-Integr. Manuf.* **46**, 114–121 (2017).
57. M. Özdemir, "Optimization in motion planning for parallel robots passing through singular positions," *J. Fac. Eng. Archit. Gazi Univ.* **32**(4), 1089–1096 (2017).
58. M. Özdemir, "Singularity analysis of two-legged planar parallel robots with three degrees of freedom," *Proc. Inst. Mech. Eng. Part C-J. Eng. Mech. Eng. Sci.* **232**(4), 657–664 (2018).
59. F. Gao, X. Liu and W. A. Gruver, "Performance evaluation of two-degree-of-freedom planar parallel robots," *Mech. Mach. Theory* **33**(6), 661–668 (1998).
60. C. M. Gosselin and J. Wang, "Singularity loci of planar parallel manipulators with revolute actuators," *Robot. Auton. Syst.* **21**(4), 377–398 (1997).
61. R. Matone and B. Roth, "In-parallel manipulators: A framework on how to model actuation schemes and a study of their effects on singular postures," *J. Mech. Des.* **121**(1), 2–8 (1999).
62. J. J. Cervantes-Sánchez, J. C. Hernández-Rodríguez and J. G. Rendón-Sánchez, "On the workspace, assembly configurations and singularity curves of the RRRRR-type planar manipulator," *Mech. Mach. Theory* **35**(8), 1117–1139 (2000).
63. G. Alıcı, "Determination of singularity contours for five-bar planar parallel manipulators," *Robotica* **18**(5), 569–575 (2000).
64. M. K. Özgören, "Motion control of constrained systems considering their actuation-related singular configurations," *Proc. Inst. Mech. Eng. Part I-J Syst Control Eng.* **215**(2), 113–123 (2001).
65. E. Macho, O. Altuzarra, C. Pinto and A. Hernandez, "Workspaces associated to assembly modes of the 5R planar parallel manipulator," *Robotica* **26**(3), 395–403 (2008).
66. R. Di Gregorio, "A novel method for the singularity analysis of planar mechanisms with more than one degree of freedom," *Mech. Mach. Theory* **44**(1), 83–102 (2009).
67. S. R. Ghorpade and B. V. Limaye, *A Course in Calculus and Real Analysis* (Springer. New York, 2006).

Appendix

$$M_{11} = m_1 g_1^2 + I_1 + m_2 \left[a_1^2 + g_2^2 + 2a_1 g_2 \cos(\theta_2 + \gamma_2)\right] + I_2 \tag{A1}$$

$$M_{12} = m_2 \left[g_2^2 + a_1 g_2 \cos(\theta_2 + \gamma_2)\right] + I_2 \tag{A2}$$

$$M_{22} = m_2 g_2^2 + I_2 \tag{A3}$$

$$M_{33} = m_3 g_3^2 + I_3 + m_4 \left[a_3^2 + g_4^2 + 2a_3 g_4 \cos(\theta_4 + \gamma_4)\right] + I_4 \tag{A4}$$

$$M_{34} = m_4 \left[g_4^2 + a_3 g_4 \cos(\theta_4 + \gamma_4)\right] + I_4 \tag{A5}$$

https://doi.org/10.1017/S0263574718000966 Published online by Cambridge University Press

$$M_{44} = m_4 g_4^2 + I_4 \tag{A6}$$

$$h_1 = m_2 a_1 g_2 \sin(\theta_2 + \gamma_2) \tag{A7}$$

$$h_2 = m_4 a_3 g_4 \sin(\theta_4 + \gamma_4) \tag{A8}$$

$$G_1 = m_1 g g_1 \cos(\theta_1 + \gamma_1) + m_2 g a_1 \cos\theta_1 + m_2 g g_2 \cos(\theta_1 + \theta_2 + \gamma_2) \tag{A9}$$

$$G_2 = m_2 g g_2 \cos(\theta_1 + \theta_2 + \gamma_2) \tag{A10}$$

$$G_3 = m_3 g g_3 \cos(\theta_3 + \gamma_3) + m_4 g a_3 \cos\theta_3 + m_4 g g_4 \cos(\theta_3 + \theta_4 + \gamma_4) \tag{A11}$$

$$G_4 = m_4 g g_4 \cos(\theta_3 + \theta_4 + \gamma_4) \tag{A12}$$

https://doi.org/10.1017/S0263574718000966 Published online by Cambridge University Press